Development of a PZT Fiber/Piezo-Polymer Composite Actuator with Interdigitated Electrodes

Cheol Kim*, Kun-Hyung Koo
Department of Mechanical Engineering, Kyungpook National University, Daegu 702-701, Korea

Piezoelectric Fiber Composites with Interdigitated Electrodes (PFCIDE) were previously introduced as an alternative to monolithic wafers with conventional electrodes for applications of structural actuation. This paper is an investigation into the performance improvement of piezoelectric fiber composite actuators by changing the matrix material. This paper presents a modified micro-electromechanical model and numerical analyses of piezoelectric fiber/piezopolymer matrix composite actuator with interdigitated electrodes (PFPMIDE). Various concepts from different backgrounds including three-dimensional linear elastic and dielectric theories have been incorporated into the present linear piezoelectric model. The rule of mixture and the modified method to calculate effective properties of fiber composites were extended to apply to the PFPMIDE model. The new model was validated when compared with available experimental data and other analytical results. To see the structural responses of a composite plate integrated with the PFPMIDE, three-dimensional finite element formulations were derived. Numerical analyses show that the shape of the graphite/epoxy composite plate with the PFPMIDE may be controlled by judicious choice of voltages, piezoelectric fiber angles, and elastic tailoring of the composite plate.

Key Words: Piezoelectric Fiber, Piezoelectric Actuator, Electrodes

1. Introduction

Recently, intelligent materials have replaced the traditional actuators and sensors. Active materials such as piezoelectrics, electrostrictives, magnetostrictives, and shape memory alloys have been investigated for a new actuator constituting smart structures (Chee et al., 1998). The conventional way of mechanical actuation in regards to the shape control of wings requires various mechanical linkages and joints (Plessis and Hagood, 1995). In particular, in aerospace industry, weight is one of the most important design constraints in so far that many efforts have been devoted to replacing the conventional heavy systems with the smart structures coupled with active materials without any functional deterioration. Piezoelectric materials are used more widely than any others, due to their high bandwidth and easy control by a voltage.

Since the piezoelectric effect was discovered by Curie brothers, Pierre and Jacques, in 1880, piezoelectric materials have evolved into several forms such as piezoceramics (Jaffe et al., 1995), piezopolymers (Gallantree, 1983), piezoelectric fibers (Hagood and Bent, 1993), piezoelectric fibrous/layer composites (Uchino, 1986; Banno, 1983; Chattopadhyay et al., 1999), and piezoelectric films. Recently, a new type of actuator called the piezoelectric fiber composite with interdigitated electrodes (PFCIDE) was introduced, and its performance, robustness, and manufacturability issues were addressed (Bent, 1997;

* Corresponding Author,
E-mail: kimchul@knu.ac.kr
TEL: +82-53-950-6586; **FAX**: +82-53-950-6550
Department of Mechanical Engineering, Kyungpook National University, Daegu 702-701, Korea. (Manuscript **Received** October 25, 2001; **Revised** January 31, 2002)

Bent and Hagood, 1997). The piezoceramic fibers maintain stiffness and bandwidth of monolithic piezoceramics and the unidirectional alignment creates orthotropic actuation. In addition, the soft matrix provides a load transfer mechanism that improves the robustness to damage and allows static ultimate tensile strength higher than monolithic ceramics. The main role of interdigitated electrodes is to ensure the uniform electric field along the fiber direction to enhance the actuation. However, the high dielectric mismatch between fiber and matrix may seriously reduce the electric field available to the fiber material actuation.

This paper investigates a way to improve the straining performance of the piezoelectric fiber composite by decreasing the dielectric mismatch between fiber and matrix through changing the matrix material from polymer to piezopolymer. The piezopolymer is flexible and has low stiffness and high damping. The two materials are quite similar in the modulus and strength, so that the change in matrix material is reasonably assumed not to cause any matrix degradation. Young's modulus of the piezopolymer is 4-6GPa (Sirohi and Chopra, 2000) and its tensile strength is 60MPa (Measurement Specialties, 1998). Generally, the modulus and tensile strength of epoxy are known to be 4.6GPa and 58.6MPa (Herakovich, 1998). A modified electromechanical model is then presented. Using the model, the effective stiffness and various constants of the piezoelectric fiber/piezoelectric polymer composite actuator with interdigitated electrodes have been calculated and compared with other data (Bent, 1997; Bent and Hagood, 1997) by a numerical analysis. In addition, in order to examine the structural responses of the PFCIDE, 3-D finite element analyses were performed for the composite plate integrated with the actuator.

2. Constitutive Equations of PZT Material

Piezoelectric materials are described by the constitutive equations given in IEEE Standards. The following forms represent the response in the material.

The stress formulation:

$$T_p = C^E_{pq} S_q - e_{kp} E_k \tag{1a}$$

$$D_i = e_{iq} S_q + \varepsilon^S_{ik} E_k \tag{1b}$$

The strain formulation:

$$S_p = S^E_{pq} T_q - d_{kp} E_k \tag{2a}$$

$$D_i = d_{iq} T_q + \varepsilon^T_{ik} E_k \tag{2b}$$

where, T_p, S_q, E_k and D_i are the material stress, the material strain, the electric field, and the electrical displacement, respectively. C^E_{pq} and ε^S_{ik} are the elastic and dielectric constants, e_{iq} and d_{iq} are the piezoelectric constants, e_{iq} describes the coupling between electric field and stress, and d_{iq} shows the coupling between electric field and strain. For example, the constant e_{33} indicates the amount of stress in the 3-direction for the given electric field in the same direction. A high value of e_{33} is desirable for increasing the actuation capability of this actuator. The superscripts of E, S and T represent constant conditional electric field, strain, and stress, respectively.

3. Micro-Electro-Mechnical Model

A number of approaches to obtain a micro-electro-mechanical model have been used to determine the effective properties. The modeling concept of the piezoelectric fiber composite with conventional electrodes and PFCIDE was first introduced in Bent et al. (1995). Previous works presented a general methodology for modeling arbitrary multi-phase materials and a combination of several uniform field cases, but these models can not be applied for active material matrix. The key to the current problem is to bring this methodology to take account of the piezoelectric fiber/piezoelectric matrix with interdigitated electrodes (PFPMIDE).

Figure 1 shows the representative volume element (RVE), a simple combination model and an approach to the PFPMIDE suggested in Bent and Hagood (1997). Three separate cases are used to capture each contribution to the overall composite response. Cases A and B assume a uniform polarization in the 3-direction. Case C is for

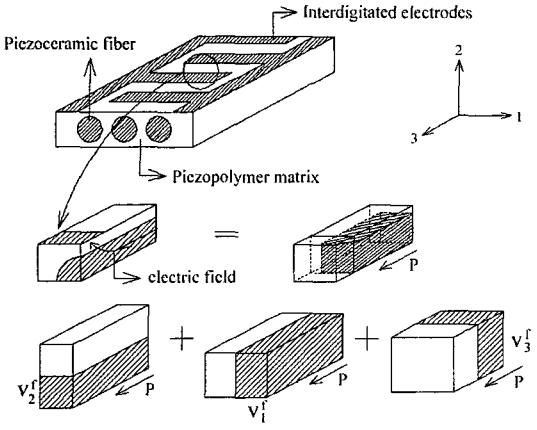

Fig. 1 Schematics of a combining process

capturing the local electrical behavior around an electrode and the field concentration in low dielectric matrix.

3.1 Case A

The modeling procedure and geometry are based on Bent and Hagood (1997). It is assumed that the mechanical and electric field are entirely uniform within each material phase so that the electromechanical shear mode problem is uncoupled from the normal mode of operation. The constitutive equations can be, therefore, represented as follows:

$$\begin{Bmatrix} T_1 \\ T_2 \\ T_3 \\ D_3 \end{Bmatrix}_f = \begin{bmatrix} C_{11}^E & C_{12}^E & C_{13}^E & -e_{31} \\ C_{12}^E & C_{22}^E & C_{32}^E & -e_{32} \\ C_{13}^E & C_{23}^E & C_{33}^E & -e_{33} \\ e_{31} & e_{32} & e_{33} & \varepsilon_{33}^S \end{bmatrix}_f \begin{Bmatrix} S_1 \\ S_2 \\ S_3 \\ E_3 \end{Bmatrix}_f \tag{3}$$

$$\begin{Bmatrix} T_1 \\ T_2 \\ T_3 \\ D_3 \end{Bmatrix}_m = \begin{bmatrix} C_{11} & C_{12} & C_{13} & -e_{31}^m \\ C_{12} & C_{22} & C_{32} & -e_{32}^m \\ C_{13} & C_{23} & C_{33} & -e_{33}^m \\ e_{31}^m & e_{32}^m & e_{33}^m & \varepsilon_{33}^m \end{bmatrix}_m \begin{Bmatrix} S_1 \\ S_2 \\ S_3 \\ E_3 \end{Bmatrix}_m \tag{4}$$

where f and m denote fiber and matrix, respectively.

Based on the uniform field assumption that means the fields are equal in the two phases, the field variables, S_1, T_2, S_3, and E_3 are equal in the two phases and regarded as independent variables in Case A. For instance, along the 1-direction, the average strain, S_1, is equal to the strain in each phase. Therefore, the above equations can be rewritten in terms of independent variables as follows:

$$T_1=\frac{1}{C_{22}^E}(C_{11}^E C_{22}^E-C_{12}^{E^2})S_1+\frac{C_{12}^E}{C_{22}^E}T_2 +\frac{1}{C_{22}^E}(C_{13}^E C_{22}^E-C_{23}^{E^2})S_3 -\frac{1}{C_{22}^E}(e_{31}C_{22}^E-e_{32}C_{12}^E)E_3 \tag{5a}$$

$$S_2=\frac{1}{C_{22}^E}(-C_{12}^E S_1+T_2-C_{23}^E S_3+e_{32}E_3) \tag{5b}$$

$$T_3=\frac{1}{C_{22}^E}(C_{13}^E C_{22}^E-C_{12}^E C_{23}^E)S_1+\frac{C_{23}^E}{C_{22}^E}T_2 +\frac{1}{C_{22}^E}(C_{33}^E C_{22}^E-C_{23}^{E^2})S_3 -\frac{1}{C_{22}^E}(e_{33}C_{22}^E-e_{32}C_{23}^E)E_3 \tag{5c}$$

$$D_3=\frac{1}{C_{22}^E}(e_{31}C_{22}^E-e_{32}C_{12}^E)S_1+\frac{e_{32}}{C_{22}^E}T_2 +\frac{1}{C_{22}^E}(e_{33}C_{22}^E-e_{32}C_{23}^E)S_3 +\frac{1}{C_{22}^E}(\varepsilon_{33}^S C_{22}^E+e_{32}^2)E_3 \tag{5d}$$

$$T_1^m=\frac{1}{C_{22}}(C_{11}C_{22}-C_{12}^2)S_1^m+\frac{C_{12}}{C_{22}}T_2^m +\frac{1}{C_{22}}(C_{13}C_{22}-C_{23}^2)S_3^m -\frac{1}{C_{22}}(e_{31}^m C_{22}-e_{32}^m C_{12})E_3^m \tag{6a}$$

$$S_2^m=\frac{1}{C_{22}}(-C_{12}S_1^m+T_2^m-C_{23}S_3^m+e_{32}^m E_3^m) \tag{6b}$$

$$T_3^m=\frac{1}{C_{22}}(C_{13}C_{22}-C_{12}C_{23})S_1^m+\frac{C_{23}}{C_{22}}T_2^m +\frac{1}{C_{22}}(C_{33}C_{22}-C_{23}^2)S_3 -\frac{1}{C_{22}}(e_{33}^m C_{22}-e_{32}^m C_{23})E_3^m \tag{6c}$$

$$D_3^m=\frac{1}{C_{22}}(e_{31}^m C_{22}-e_{32}^m C_{12})S_1^m+\frac{e_{32}{}^m}{C_{22}}T_2^m +\frac{1}{C_{22}}(e_{33}^m C_{22}-e_{32}^m C_{23})S_3^m +\frac{1}{C_{22}}(\varepsilon_{33}^m C_{22}+e_{32}^{m^2})E_3^m \tag{6d}$$

By using the rule of mixture, the above equations can be rewritten in a compact form:

$$\begin{Bmatrix} \bar{T}_1 \\ \bar{S}_2 \\ \bar{T}_3 \\ \bar{D}_3 \end{Bmatrix} = v_2^f \begin{Bmatrix} T_1 \\ S_2 \\ T_3 \\ D_3 \end{Bmatrix}_f + v_2^m \begin{Bmatrix} T_1 \\ S_2 \\ T_3 \\ D_3 \end{Bmatrix}_m \tag{7}$$

where v_2^f is the fraction of piezoelectric fiber s measured across the element in the 2-direction and the affer bar means average value.

Rewriting the above equation in its original form yields:

$$\begin{Bmatrix} \bar{T}_1 \\ \bar{T}_2 \\ \bar{T}_3 \\ \bar{D}_3 \end{Bmatrix} = \begin{bmatrix} C_{11}^{eff} & C_{12}^{eff} & C_{13}^{eff} & -e_{31}^{eff} \\ C_{12}^{eff} & C_{22}^{eff} & C_{23}^{eff} & -e_{32}^{eff} \\ C_{13}^{eff} & C_{23}^{eff} & C_{33}^{eff} & -e_{33}^{eff} \\ e_{31}^{eff} & e_{32}^{eff} & e_{33}^{eff} & \varepsilon_{33}^{eff} \end{bmatrix} \begin{Bmatrix} \bar{S}_1 \\ \bar{S}_2 \\ \bar{S}_3 \\ \bar{E}_3 \end{Bmatrix} \tag{8}$$

where:

$$C_{11}^{eff} = (v_2^f C_{11}^E + v_2^m C_{11}) - \frac{v_2^f v_2^m (C_{12}^E - C_{12})^2}{v_2^f C_{22} + v_2{}^m C_{22}^E}$$

$$C_{12}^{eff} = \frac{v_2^f C_{12}^E C_{22} + v_2^m C_{12} C_{22}^E}{v_2^f C_{22} + v_2^m C_{22}^E}$$

$$C_{13}^{eff} = (v_2^f C_{13}^E + v_2^m C_{13}) - \frac{v_2^f v_2^m (C_{12} - C_{12}^E)(C_{23} - C_{23}^E)}{v_2^f C_{22} + v_2^m C_{22}^E}$$

$$C_{22}^{eff} = \frac{C_{22}^E + C_{22}}{v_2^f C_{22} + v_2^m C_{22}^E} \tag{9a}$$

$$C_{23}^{eff} = \frac{v_2^f C_{23}^E C_{22} + v_2^m C_{23} C_{22}^E}{v_2^f C_{22} + v_2^m C_{22}^E}$$

$$C_{33}^{eff} = (v_2^f C_{33}^E + v_2^m C_{33}) - \frac{v_2^f v_2^m (C_{23} - C_{23}^E)^2}{v_2^f C_{22} + v_2^m C_{22}^E}$$

$$e_{31}^{eff} = (v_2^f e_{31} + v_2^m e_{31}^m) - \frac{v_2^f v_2^m (e_{32}^m - e_{32})(C_{12} - C_{12}^E)}{v_2^f C_{22} + v_2^m C_{22}^E}$$

$$e_{32}^{eff} = \frac{v_2^f e_{32} C_{22} + v_2^m e_{32}^m C_{22}^E}{v_2^f C_{22} + v_2^m C_{22}^E} \tag{9b}$$

$$e_{33}^{eff} = (v_2^f e_{33} + v_2^m e_{33}^m) - \frac{v_2^f v_2^m (C_{23} - C_{23}^E)(e_{32}^m - e_{32})}{v_2^f C_{22} + v_2^m C_{22}^E}$$

$$e_{33}^{eff} = (v_2^f \varepsilon_{33}^S + v_2^m \varepsilon_{33}^m) - \frac{v_2^f v_2^m (e_{32}^m - e_{32})^2}{v_2^f C_{22} + v_2^m C_{22}^E} \tag{9c}$$

3.2 Case B

Since the composite actuator is symmetric about the axis 3 and the direction of polarization is assumed to be uniform along the length of the fiber, the constitutive equations for Case B are easily obtained by interchanging the subscripts "1" and "2" in both the effective and constitutive properties of the previous equations.

$$\begin{aligned} &C_{11}^{eff} \rightarrow C_{22}^{eff},\ C_{22}^{eff} \rightarrow C_{11}^{eff},\ C_{13}^{eff} \rightarrow C_{23}^{eff} \\ &C_{23}^{eff} \rightarrow C_{13}^{eff},\ C_{31}^{eff} \rightarrow C_{32}^{eff},\ C_{32}^{eff} \rightarrow C_{31}^{eff} \end{aligned} \tag{10}$$

3.3 Case C

Case C is to consider the interdigitated of a piece of the interdigited electrode. Since the matrix was not an active material in the previous model (Bent and Hagood, 1997), the mechanical field of the matrix was not considered in the model. However, this study uses an active material for the matrix, so that the previous model cannot be applied and needs to be modified. A modified model applicable to both active and inactive matrix materials is developed in this study.

Now, the independent variables in Case C are S_1, S_2, T_3, and D_3. As the method of deriving effective properties is similar to Case A, the constitutive equation can be expressed as follows:

$$\begin{Bmatrix} \bar{T}_1 \\ \bar{T}_2 \\ \bar{S}_3 \\ \bar{E}_3 \end{Bmatrix} = v_3^f \begin{Bmatrix} T_1 \\ T_2 \\ S_3 \\ E_3 \end{Bmatrix}_f + v_3^m \begin{Bmatrix} T_1 \\ T_2 \\ S_3 \\ E_3 \end{Bmatrix}_m \tag{11}$$

$$\begin{Bmatrix} \bar{T}_1 \\ \bar{T}_2 \\ \bar{T}_3 \\ \bar{D}_3 \end{Bmatrix} = \begin{bmatrix} C_{11}^{eff} & C_{12}^{eff} & C_{13}^{eff} & -e_{31}^{eff} \\ C_{12}^{eff} & C_{22}^{eff} & C_{23}^{eff} & -e_{32}^{eff} \\ C_{13}^{eff} & C_{23}^{eff} & C_{33}^{eff} & -e_{33}^{eff} \\ e_{31}^{eff} & e_{32}^{eff} & e_{33}^{eff} & \varepsilon_{33}^{eff} \end{bmatrix} \begin{Bmatrix} \bar{S}_1 \\ \bar{S}_2 \\ \bar{S}_3 \\ \bar{E}_3 \end{Bmatrix} \tag{12}$$

3.4 Combined model

The order in which each case is coupled in the combined model is C → A → B. In other words, the sequence that effective properties of case C are substituted into the piezoelectric fiber properties of case A which then are substituted into the piezoelectric fiber properties of case C, yielding the effective properties of the combined model. This combining order can accurately reflect the fact that the electric field in a fiber is more influenced by the matrix between the fiber and the electrode, rather than the matrix at any other points.

Figure 2 shows the actual PFPMIDE geometry. Here, the relationship between a fiber volume fraction v^f, and a line fraction X, is described. When a circular fiber is idealized as a square, it is simply assured that the area of a square fiber be

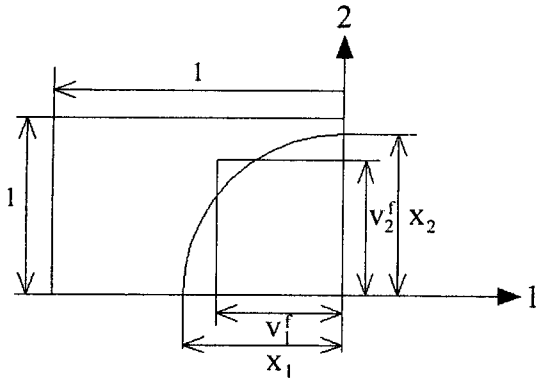

Fig. 2 Geometry of an actual PFPMIDE model

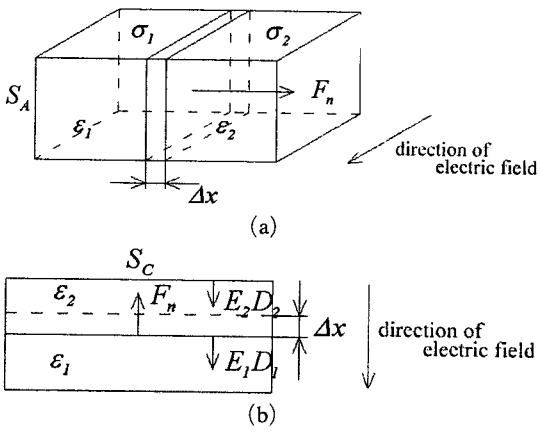

Fig. 3 Direction of the interface force depending on the direction of an electric field

the same as that of a circular fiber using the fiber volume fraction, v^f. This can be expressed as follows:

$$v^f = v_1^f v_2^f = \frac{\pi}{4} X_1 X_2 \text{ when } v_1^f = v_2^f \tag{13}$$

where X_1 and X_2 are called the fiber line fractions of an actual circular fiber composite.

The piezoceramic fiber volume fraction v_3^f i n case C represents the portion of ceramics along the electric field path length. It is a function of the fiber volume fraction in the 2-direction and the geometry of interdigitated electrode pattern. This can be represented as a following equation:

$$v_3^f = \frac{p/2}{p/2 + (h/2)\, v_2^m} = \frac{p/h}{p/h + (1 - v_2^f)} \tag{14}$$

where p is a space between electrodes and h is a wafer thickness.

4. Interface Forces Between Fiber and Matrix

The interface forces that occur due to the dielectric mismatch between fiber and matrix of a PFPMIDE need to be considered, which is not the case in a monolithic PZT plate. Figure 3 depicts the direction of the interface force depending on the direction of an electric field.

When the direction of an electric field is parallel to the interface as in Fig. 3(a), the interface force F_n is derived based on the following procedure. Based on the principle of virtual displacement, the energy change ΔW_2 in a small region Δx as in Fig. 3 is given by before displacement:

$$\Delta W_2 = \frac{1}{2} E_2 D_2 S_A \Delta x \tag{15}$$

After displacement, the energy change ΔW_1 is given by:

$$\Delta W_1 = \frac{1}{2} E_1 D_1 S_A \Delta x \tag{16}$$

where E, D, and S denote the electric flux, the electric flux density, and the cross-sectional area, respectively.

The derivation of an electric force, F_n, can be facilitated by considering the energy changes originated from the variation in the electric charge density due to interface straining. At the interface, E_1 equals to E_2 because two are parallel $D_1 \neq D_2$ due to $\varepsilon_1 \neq \varepsilon_2$. Under the conditions of $D_1 = \sigma_1$, $D_2 = \sigma_2$ the energy difference in Δx before and after displacement is given by:

$$V(\sigma_2 - \sigma_1)\Delta x = V(D_2 - D_1)\Delta x \tag{17}$$

where σ denotes the electric energy density.

The mechanical energy needed to move the interface, $F_n S_A \Delta x$, can be written in the form:

$$F_n S_A \Delta x = \Delta W_2 - \Delta W_1 - V(D_2 - D_1)\Delta x \tag{18}$$

where V denotes the voltage. Using the relationship, $V = E_1 d = E_2 d$, Eq. (18) can be rewritten as:

$$F_n S_A \Delta x = \left\{ \frac{1}{2} E_2 D_2 - \frac{1}{2} E_1 D_1 + E_1 D_1 - E_2 D_2 \right\} S_A \Delta x \tag{19}$$

The final form F_n can be expressed as:

$$F_n=\frac{1}{2}E_1D_1-\frac{1}{2}E_2D_2 \\ =\frac{1}{2}(\varepsilon_1-\varepsilon_2)E^2[\mathrm{N/m^2}] \tag{20}$$

where $E_1=E_2=E$. Since the dielectric constant of a fiber is larger than that of matrix, the force acts toward matrix from fiber.

When the direction of an electric field is orthogonal to the interface as in Fig. 3(b), the energy change in Δx before displacement is expressed as

$$\Delta W_2=\frac{1}{2}E_2D_2S_C\Delta x \tag{21}$$

After displacement,

$$\Delta W_1=\frac{1}{2}E_1D_1S_C\Delta x \tag{22}$$

The force caused by the change in energy can be explicitly written as follows:

$$F_n=S_C\Delta x=\Delta W_2-\Delta W_1 \tag{23}$$

Finally,

$$F_n=\frac{1}{2}E_2D_2-\frac{1}{2}E_1D_1 \\ =\frac{1}{2}\left(\frac{1}{\varepsilon_2}-\frac{1}{\varepsilon_1}\right)D^2[\mathrm{N/m^2}] \tag{24}$$

where $D_1=D_2=D$, $E_2=D/\varepsilon_2$, and since the dielectric constant of a fiber is larger than that of matrix, the fiber attracts matrix in this case.

5. Finite Element Formulation

The 8-noded incompatible solid element was used to study the structural behaviors in this paper. Based on the principle of the minimum potential energy, the governing equation for PFPMIDE and graphite/epoxy composite body (Π) is given by:

$$\int_{\Pi}\tilde{\sigma}\cdot\delta\tilde{\varepsilon}d\Pi-\int_{\Pi}f\cdot\delta ud\Pi-\int_{\Gamma}t\cdot\delta uds=\min \tag{25}$$

where $\tilde{\sigma}$, $\tilde{\varepsilon}$, f, u, t, and Γ are stress, strain, body force, displacement, surface traction, and applied force boundary, respectively. The strain is defined in terms of the displacement as:

$$2\tilde{\varepsilon}=\nabla u+(\nabla u)^T \tag{26}$$

where ∇ is the gradient operator.

The coordinates X and displacements u can be expressed as follows using interpolation functions:

$$x=\begin{Bmatrix}X\\Y\\Z\end{Bmatrix}=\sum_{i=1}^{8}\psi_i x_i, \\ u=\begin{Bmatrix}u_X\\u_Y\\u_Z\end{Bmatrix}=\sum_{i=1}^{8}\psi_i u_i+\sum_{i=1}^{3}\tilde{S}_i a_i \tag{27}$$

and the shape functions are defined as follows:

$$\psi_i(\xi,\eta,\zeta)=\frac{1}{8}(1+\xi_i\xi)(1+\eta_i\eta)(1+\zeta_i\zeta)\ i=1,\cdots,8 \\ \tilde{S}_1=1-\xi^2,\ \tilde{S}_2=1-\eta^2,\ \tilde{S}_3=1-\zeta^2 \tag{28}$$

where the symbols ξ, η, and ζ are the natural coordinates, the values ξ_i, η_i, and ζ_i are obtained at each node. $\tilde{S}_i$ is a bubble function which reflects the incompatible mode. The incompatible mode a has the same effect as adding more nodes.

From Eqs. (26) and (28), the strain is expressed as:

$$\tilde{\varepsilon}=\sum_{i=1}^{8}B_iu_i+\sum_{i=1}^{3}G_ia_i \tag{29}$$

where,

$$\tilde{\varepsilon}=\begin{bmatrix}\varepsilon_{xx}\\\varepsilon_{yy}\\\varepsilon_{zz}\\\gamma_{yz}\\\gamma_{xz}\\\gamma_{xy}\end{bmatrix},\ B_i=\begin{bmatrix}\psi_{i,1}&0&0\\0&\psi_{i,2}&0\\0&0&\psi_{i,3}\\0&\psi_{i,3}&\psi_{i,2}\\\psi_{i,3}&0&\psi_{i,1}\\\psi_{i,2}&\psi_{i,1}&0\end{bmatrix},\ G_i=\begin{bmatrix}S_{i,1}&0&0\\0&S_{i,2}&0\\0&0&S_{i,3}\\0&S_{i,3}&S_{i,2}\\S_{i,3}&0&S_{i,1}\\S_{i,2}&S_{i,1}&0\end{bmatrix} \tag{30}$$

Eq. (25) is expressed as a following discrete function:

$$\begin{bmatrix}K^e_{uu}&K^e_{ua}\\K^e_{au}&K^e_{aa}\end{bmatrix}\begin{Bmatrix}u^e\\a^e\end{Bmatrix}=\begin{Bmatrix}F^e\\0\end{Bmatrix} \tag{31}$$

where,

$$F^e=\int_{\Gamma^e}H^TtdS \tag{32}$$

$$K^e_{uu\ddot{v}}=\int_{Ve}B_i^TDB_jdV,\ K^e_{ua\ddot{v}}=\int_{Ve}B_i^TDG_jdV \\ K^e_{au\ddot{v}}=\int_{Ve}G_i^TDB_jdV,\ K^e_{aa\ddot{v}}=\int_{Ve}G_i^TDG_jdV \tag{33}$$

and the interpolation matrix H is given by

$$H=\begin{bmatrix} \psi_1 & 0 & 0 & \cdots & \psi_8 & 0 & 0 \\ 0 & \psi_1 & 0 & \cdots & 0 & \psi_8 & 0 \\ 0 & 0 & \psi_1 & \cdots & 0 & 0 & \psi_8 \end{bmatrix} \quad (34)$$

The nodeless D.O.F., a in the lower of Eq. (31) can be rewritten in the form:

$$\{a^e\}=-[K_{aa}^e]^{-1}[K_{au}^e]\{u^e\} \quad (35)$$

Substituting this into Eq. (31) gives:

$$[K^e]=[K_{uu}^e]-[K_{ua}^e][K_{aa}^e]^{-1}[K_{au}^e] \quad (36)$$

Adding all elements results in the following governing equation:

$$\Sigma K^e U=\Sigma F^e \quad (37)$$

6. Results and Discussions

The numerical results of the effective stiffness from the current and Hagood's models are plotted in Figs. 4 and 5 in order to demonstrate the versatility of the modified model. Good correlations between the two results mean that the current model is applicable to the piezo-fiber composite actuators with both active and inactive matrix materials. On the other hand, the other can be only applied to the actuator with inactive matrix, which consists of PZT5H fiber and hybrid matrix. Material properties used in the validation studies are listed in Table 1. The three different results obtained under the same environment are shown in Fig. 5. In this figure, the fiber thickness line fraction, X_2, was held in the range of 0.909 to 0.942 for all three cases. The experimental data were excerpted from Bent and Hagood (1997) and the results shown here are in a quite good agreement.

Table 1 Properties of actuator materials

	PZT 5H fibers	Copoly-mer	Hybrid matrix	Epoxy
C_{11}^E (Gpa)	127	7.98	8.15	5.14
C_{12}^E (Gpa)	80.2	5.10	4.01	2.77
C_{13}^E (Gpa)	84.7	5.10	4.01	2.77
C_{33}^E (Gpa)	117	7.98	8.15	5.14
e_{31} (c/m^2)	−4.42	−0.05	0	0
e_{33} (c/m^2)	15.5	0.19	0	0
$\varepsilon_{33}^S/\varepsilon_0$	1392	8.0	11.2	4.0

The correlations between effective piezoelectric constants predicted by the modified model of the PZT fiber/piezopolymer actuator and those predicted by the non-active mode. are shown in Fig. 6. It can be seen that because the piezo-electricity of matrix can not be considered by the non-active Hagood model, the errors between

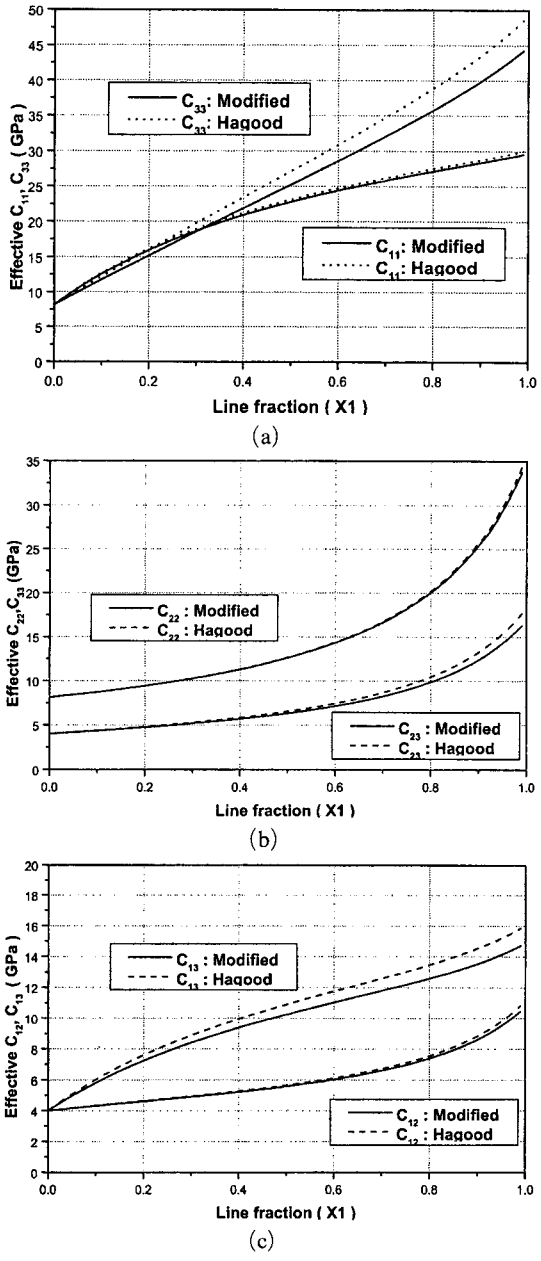

Fig. 4 Effective stiffness of a PZT 5H fiber/hybrid matrix actuator

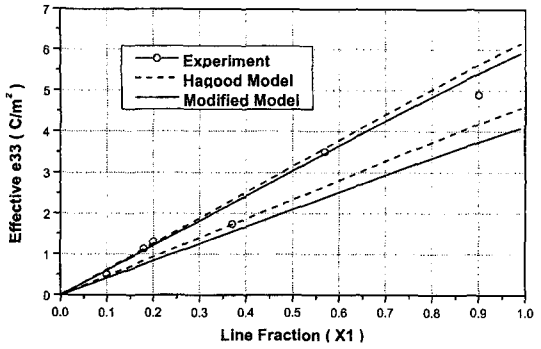

Fig. 5 Effective piezoelectric constants of a PZT 5H fiber/hybrid matrix actuator

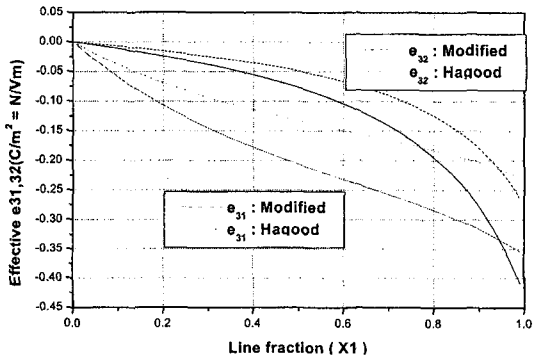

Fig. 6 Effective piezoelectric constants of a PZT 5H fiber/piezopolymer matrix actuator

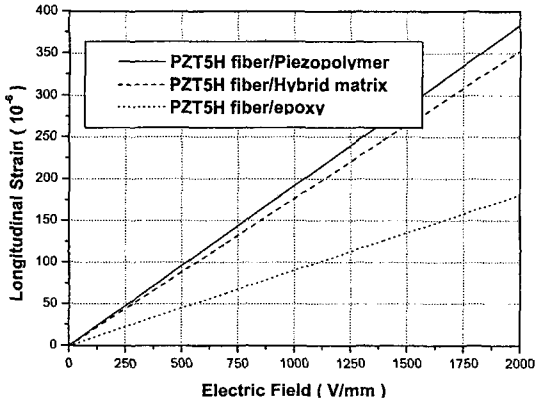

Fig. 7 Performance comparison of piezoelectric fiber composite actuators

two are large when increasing the line fraction. Fig. 7 shows the fiber-directional strain of the PFPMIDE actuator which is its main actuating force index due to the IDE is larger than any others. The actuating force of the PFPMIDE

Table 2 Mechanical properties of graphite/epoxy

E1=155 Gpa	E2=E3=12.10 Gpa
G23=3.20 GPa	G12=G13=4.40
ν_{23}=0.458	$\nu_{12}=\nu_{13}$=0.258

Table 3 Plate dimensions (mm)

Length (L)	63.5
Width (W)	14
Thickness (t_1)	0.145
Thickness (t_2)	0.125

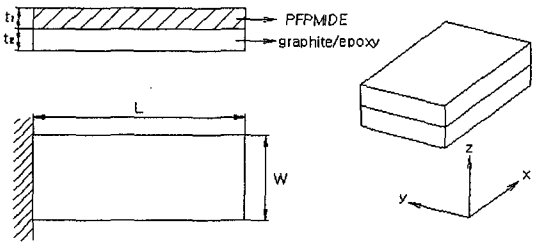

Fig. 8 Schematic of a PFPMIDE and graphite/epoxy

actuator is as high as twice compared to the one with epoxy matrix and is 10% higher than Hagood's (i.e., PZT5H fiber/hybrid matrix). These results indicate that the performance and the dielectric mismatch can be improved by using an active matrix material such as piezopolymer.

Finite element analyses have been carried out using 3-dimensional brick elements to investigate the possible applications to the shape control of thin plate structures integrated with a PFPMIDE/graphite/epoxy composite actuator. The plate feature used in this study is shown in Fig. 8. The material properties of PZT5H, piezopolymer, and graphite/epoxy are listed in Table 1 and 2. The plate geometries used are shown in Table 3. The 0 degree of the actuator and four different stacking sequences of graphite/epoxy, $\alpha(0°, 30°, 45°, 90°)$ have been investigated. The plate was modeled using 400 brick elements. Figsures 9 and 10 shows the deformations of the structure depending on the electric fields. The largest longitudinal elongation is occurred at [0°/90°] because the stiffness effect of graphite fibers is negligibly small in this case. Due to different stiffnesses between the actuator and

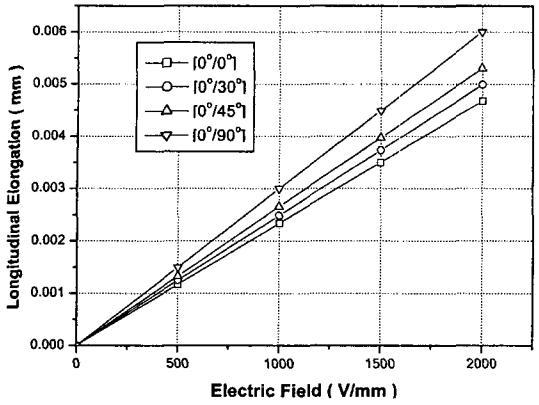

Fig. 9 Longitudinal elongation of a composite plate with PFPMIDE

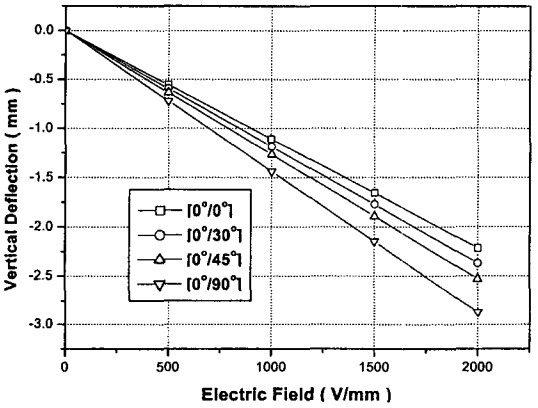

Fig. 10 Bending deflection of a composite plate with PFPMIDE

composites, the electric field causes the largest bending deflection at [0°/90°]. The largest bending deflection in Fig. 10 shows to be approximately twice compared to the THUNDER. The structural responses of the plate indicate that the judicious choice of the lay-up sequence and the electric field could improve the performance of the current PFPMIDE actuator.

7. Conclusions

A new method which can improve the performance of a piezoelectric fiber composite actuator and reduce the dielectric mismatch by the application of various matrix materials was presented in this paper. A micro-electromechanical model as a modified model has been proposed and employed to predict the effective material properties of the new PFPMIDE actuator. The modified model shows good agreements with other analytical results and experimental data, which validates the use of this approach to predict various effective piezoelectric properties. Hence the modified model demonstrated its versatility through comparisons with other results. The excellent correlation determines its applicability to the piezo-fiber composite actuators with both active and inactive matrix materials.

To investigate the structural responses of a composite plate with a PFPMIDE actuator, three-dimensional finite element formulations were derived. Numerical analyses show that the shapes of graphite/epoxy composite plates with the improved PFPMIDE could be controlled by the judicious choice of voltages, PZT fiber angles, and elastic tailoring of the composite plates.

References

Banno, H., 1983, "Recent Developments of Piezoelectric Ceramic Products and Composites of Synthetic Rubber and Piezoelectric Ceramic Particles," *Ferroelectrics*, Vol. 50, pp. 3~12.

Bent, A. A., 1997, "Active Fiber Composite for Structural Actuation," Ph. D. thesis, MIT.

Bent, A. A. and Hagood, N. W., 1997, "Piezoelectric Fiber Composites with Interdigitated Electrodes," *Journal of Intelligent Material Systems and Structures*, Vol. 8, pp. 903~919.

Bent, A. A., Hagood, N. W. and J. P. Rodgers, 1995, "Anisotropic Actuation with Piezoelectric Fiber Composites," *Journal of Intelligent Material Systems and Structures*, Vol. 6, No. 3, pp. 338~349.

Chattopadhyay, A., Li, J. and Gu, H., 1999, "Coupled Thermo-Piezoelectric-Mechanical Model for Smarts Composite Laminates," *AIAA Journal*, Vol. 37, No. 12, pp. 1633~1638.

Chee, C. Y. K., Tong, L. and Steven, G. P., 1998, "A Review on the Modeling of Piezoelectric Sensor and Actuators Incorporated in Intelligent Structures," *Journal of Intelligent Material Systems and Structures*, Vol. 9, pp. 3~19.

Gallantree, H. R., 1983, "Review of Transducer Applications of Polyvinylidene Fluoride," IEE proceedings 130, pp. 219~224.

Hagood, N. W. and Bent, A. A., 1993, "Development of Piezoelectric Fiber Composites for Structural Actuation," AIAA Paper No. 93-1717, Proceedings of 34th AIAA Structures, Structural Dynamics, and Materials Conference, La Jolla, CA.

Herakovich, C. T., 1998, *Mechanics of Fibrous Composites*, John Wiley & Sons, Inc.

IEEE Std 176-1978, *IEEE Standard on Piezoelectricity*, The Institute of Electrical and Electronics Engineers.

Jaffe, B., Roth, R. S. and Marzullo, S., 1995, "Properties of Piezoelectric Ceramics in the Solid-Solution Series Lead Titanate-Lead Zirconate-Lead Oxide: Tin Oxide and Lead Titanate-Lead Hanate," *Journal of Research of the National Bureau of Standards* 55, pp. 239~254.

Measurement Specialties, Inc., 1998, *Piezo Film Sensors Technical Manual, Part 5 of 18*.

Plessis, A. J. D. and Hagood, N. W., 1995, "Performance Investigation of Twist Actuated Single Cell Composite Beams for Helicopter Blade Control," 6th International Conference on Adaptive Structures and Technology, Key West, FL.

Sirohi, J. and Chopra, I., 2000, "Fundamental Understanding of Piezoelectric Strain Sensors," *Journal of Intelligent Material Systems and Structures*, Vol. 11, pp. 246~257.

Taylor, R. L., Beresford, P. J. and Wilson, E. L., 1976, "A Non-Conforming Element for Stress Analysis," *International Journal for Numerical Methods in Engineering*, Vol. 10, No. 6, pp. 1211~1219.

Uchino, K., 1986, "Electrostrictive Actuators: Materials and Applications," American Ceramic Society Bulletin 65, pp. 647~652.